THE JOURNAL OF PHYSICAL CHEMISTRY B

Article

pubs.acs.org/JPCB

Effective Surface Coverage of Coarse-Grained Soft Matter

Galen T. Craven, Alexander V. Popov, and Rigoberto Hernandez*

Center for Computational Molecular Science and Technology, School of Chemistry and Biochemistry, Georgia Institute of Technology, Atlanta, Georgia 30332-0400, United States

ABSTRACT: The surface coverage of coarse-grained macromolecules bound to a solid substrate is not simply proportional to the two-dimensional number density because macromolecules can overlap. As a function of the overlap probability δ, we have developed analytical formulas and computational models capable of characterizing this nonlinear relationship. For simplicity, we ignore site−site interactions that would be induced by length-scale mismatches between binding sites and the radius of gyration of the incident coarse-grained macromolecular species. The interactions between macromolecules are modeled with a finite bounded potential that allows multiple macromolecules to occupy the same binding site. The softness of the bounded potential is thereby reduced to the single parameter δ. Through variation of this parameter, completely hard ($\delta = 0$) and completely soft ($\delta = 1$) behavior can be bridged. For soft macromolecular interactions ($\delta > 0$), multiple occupancy reduces the fraction of sites ϕ occupied on the substrate. We derive the exact transition probability between sequential configurations and use this probability to predict ϕ and the distribution of occupied sites. Due to the complexity of the exact ϕ expressions and their analytical intractability at the thermodynamic limit, we apply a simplified mean-field (MF) expression for ϕ. The MF model is found to be in excellent agreement with the exact result. Both the exact and MF models are applied to an example dynamical system with multibody interactions governed by a stochastic bounded potential. Both models show agreement with results measured from simulation.

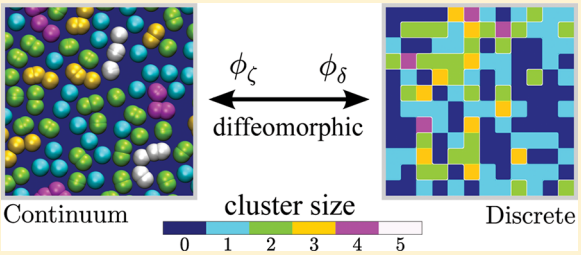

1. INTRODUCTION

The phase and spatial behavior observed in the assembly of a monomeric species into oligomeric clusters[1−7] drives the design of materials with unique functionalities.[8−11] At atomistic length scales, the structural complexity arising from assembly is often difficult to describe using analytical theory or to simulate on relevant time scales due to the large numbers of degrees of freedom that constitute such systems. To reduce this complexity, the atomistic degrees of freedom can be reduced to a coarse-grained (CG) description where a group of atomic degrees of freedom is mapped onto a single CG site.[12−16] At mesoscopic length scales, CG macromolecules can be modeled using repulsive potentials that are finite valued at the origin, i.e., bounded potentials.[17,18] The finite nature of bounded interactions allows for multiple macromolecules to overlap and occupy the same volume in configuration space.[19,20] Studies of mesoscopic systems with interactions dictated by bounded potentials include colloid suspensions,[21] polymer−colloid mixtures,[22] star polymers,[23] and block copolymers.[24,25]

The structures that emerge from overlapping spatial configurations render nontrivial geometries of the system's particle phase. This is in contrast to the atomistic scale in which nuclear repulsion does not allow for pairs of atoms to overlap, and thus mutually exclusive probabilistic arguments suffice to describe the resulting bulk-phase structure. This overlapping phenomenon has been observed experimentally in the structure factor of dendrimers, measured with small-angle neutron scattering[26] in agreement with the theoretical predictions of Likos and co-workers.[20,27]

The determination of the occupied volume fraction of a system's particle phase ϕ is of specific interest for the design of materials with properties driven by bulk-phase connectivity, such as conductivity and permeability.[28−34] The attainable particle-phase volume fraction in systems consisting of soft macromolecular structures is much larger than that of systems governed by hard core (HC) potentials.[35] In simple HC models, such as the well-known hard sphere systems,[36] the infinite value of the governing potentials prohibits a set of particles from overlapping. When coarse-grained intermolecular interactions are modeled using bounded potentials, an increase in attainable volume fractions gives rise to complex clustering behavior,[20,37−40] as the particles are allowed to overlap relative to their characteristic radius of gyration.

The assembly of particles on a substrate that are prohibited from overlapping because of steric repulsion is often modeled using random sequential adsorption (RSA).[41] In the RSA procedure, particles are deposited sequentially, with the position of the incident particle chosen at random. If the placement of an incident particle on the chosen position leads to overlap with any previously added particle, the particle does not bind to the substrate. The insertion of nonoverlapping objects to a volume generates nonequilibrium structures that differ from the configurations generated by HC systems in

Special Issue: Spectroscopy of Nano- and Biomaterials Symposium

Received: May 27, 2014
Revised: July 22, 2014
Published: July 24, 2014

dx.doi.org/10.1021/jp505207h | J. Phys. Chem. B 2014, 118, 14092−14102

thermodynamic equilibrium.[42,43] By forming geometrical objects through combinations of identical spheres, RSA can be extended to polymeric structures.[44,45]

The RSA can be further generalized through the random site model (RSM) by subdividing the substrate into a random distribution of discretized binding sites.[46,47] The occupied fraction of independent discrete sites, when only monolayers are allowed, can then be obtained from the standard Langmuir isotherm.[48] Multilayer coverage and distributions in reversible equilibrium adsorption processes can be addressed through the BET (Brunauer, Emmett, and Teller) isotherm[49] as long as adsorbate−adsorbate interactions are ignorable.[50]

In the deposition of coarse-grained macromolecules on a surface, there is a possibility for them to occupy the same binding site at a finite energy cost, and this can be addressed even within interaction models that involve bounded potentials. The single occupancy criterion of the RSM and the Langmuir isotherm does not sufficiently describe the complexity of the generated structures with such multiple occupancy. Multilayer isotherms built on assumptions involving bulk-phase interactions and the independence of each monolayer also fail. Finken et al.[51] and Likos et al.[52] have developed multiple occupancy lattice models to study the phase behavior of coarse-grained macromolecules through evaluation of approximated partition functions. These studies have elucidated both phase separations and the transition to clustering regimes in equilibrium CG systems, but they are not directly applicable to the prediction of structures generated from sequential addition processes.

The self-organization of cells on microstructured surfaces is another example of an observed multiple occupancy phenomenon. Binding sites are created by coating a substrate with protein. A cell line is introduced to the substrate and the cells self-organize on the binding sites. After organization, a fraction of lattice sites will be occupied by multiple cells.[53] Multiple occupancy is advantageous for processes in which cell-to-cell communication drives survival and function[54] but also a hindrance to the creation of single cell assays.

In this article, we use an avoidance-modified soft sequential adsorption (SSA) algorithm to model coarse-grained macromolecules binding to a substrate. It takes advantage of our recent model[33,34] treating soft (penetrable) interactions using stochastic hard-sphere potentials. In the SSA process, purely repulsive pairwise interactions drive the assembly, and the bounded nature of the underlying potential allows multiple molecular structures to occupy the same binding site. Simulations and a new theoretical framework of the SSA process provide the fraction of occupied binding sites ϕ and the distribution of occupied sites. For systems at the thermodynamic limit, we derive ϕ using mean field (MF) arguments and compare both the exact and MF results with measurements taken from Monte Carlo (MC) simulations, with excellent agreement observed. These expressions are applied to a system governed by a stochastic bounded potential that includes multibody interactions. We find that using the exact SSA derivation of ϕ, we can predict the occupied volume fraction of equilibrium configurations of coarse-grained, penetrable systems. The occupied volume fraction also differs from what is observed in the case of relaxed surface coverage (RSC), that is, when the particles are allowed to move between binding sites upon SSA.

2. SOFT SEQUENTIAL ADSORPTION (SSA)

We consider a substrate with n discrete binding sites and k incident macromolecules, which arrive sequentially and bind irreversibly to the substrate. The potential between a pair of macromolecules, i and j, is described by

$$V(r_{ij}) = \begin{cases} \epsilon, & r_{ij} = 0 \\ 0, & \text{otherwise} \end{cases} \tag{1}$$

which is ϵ if the pair of macromolecules occupies the same site on the substrate and 0 otherwise. A potential of this form is a lattice generalization of the well-known penetrable sphere (PS) potential[55−59] introduced by Marquest and Whitten,[60] to model solutions of micelles.

Through the introduction of a Boltzmann weighted softness parameter

$$\delta = \mathrm{e}^{-\epsilon^*} \tag{2}$$

with $\epsilon^* = \epsilon/k_\mathrm{B}T$, the softness of the underlying potential can be reduced to one parameter. The limiting values of this parameter classify the adsorbate as completely hard ($\delta = 0$) when no multiple occupancy is allowed and as completely soft ($\delta = 1$) when macromolecules are allowed to occupy the same binding site. For a particular system, the actual value of δ would depend on, for example, the critical adsorption point, internal structure, orientation, and chain length of the incident species.[61,62] At intermediate values, $0 < \delta < 1$, complex structures are generated through the non-Markovian, avoidance-modified SSA algorithm, which is implemented as follows:

1. *A substrate with n binding sites is created and a value of the softness parameter $\delta \in [0, 1]$ is preassigned to the incident binding macromolecules.*
2. *A macromolecule is created and a binding site on the substrate is selected randomly from a uniform distribution.*
3. *If the binding site is unoccupied, the macromolecule irreversibly adsorbs to the selected site. Bound macromolecules do not diffuse on the surface or desorb from the surface.*
4. *If the binding site is already occupied by $i > 0$ macromolecules, the macromolecule irreversibly adsorbs to the selected site with probability δ^i and is rejected from the site with probability $(1 - \delta^i)$.*
5. *If the macromolecule is rejected from the binding site, a new binding site on the substrate is selected randomly, with all sites having equal probability of being selected, and the acceptance loop (steps 3 and 4) is repeated.*

The sequential creation−acceptance process is repeated until k macromolecules are added to the substrate. After the sequential addition of macromolecules, the substrate will have some number of occupied and unoccupied sites. The occupied volume fraction ϕ is the average number of occupied binding sites, i.e., the surface coverage concentration.

The number of possible microstates for a lattice system that allows multiple occupancy, where both the macromolecules and binding sites are distinguishable, is n^k. The energy of the system

$$E = \sum_{i=1}^{k} \sum_{i>j} V(r_{ij}) \tag{3}$$

is characterized entirely by the intermolecular interactions. It is notable that the distribution of energy states generated by sequential addition methods cannot be equated to the

dx.doi.org/10.1021/jp505207h | J. Phys. Chem. B 2014, 118, 14092−14102

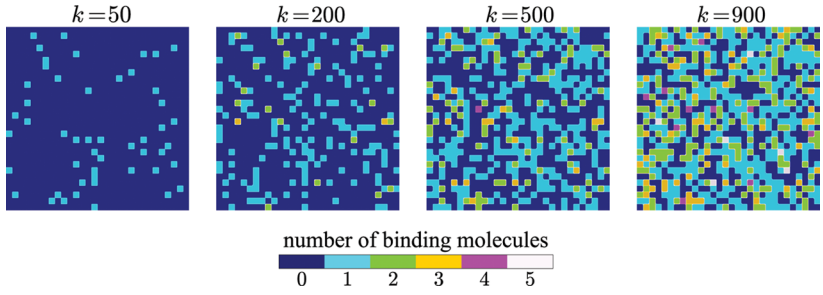

Figure 1. Several configurations generated as k = 900 macromolecules are sequentially added to solid substrate with n = 900 binding sites. The softness parameter is δ = 1. Each binding site is colored according to the number of particles that occupy that site. The configurations shown are progressive; each configuration c is built from the one before $c_{50} \rightarrow c_{200} \rightarrow c_{500} \rightarrow c_{900}$.

probabilistic distribution of the canonical Boltzmann partition function.[42]

In this article, we will derive methods to predict the weighting of microstates that arise from the SSA procedure. Through calculation of the microstate weighting, either by exact means or through approximate methods, spatial properties of a system undergoing SSA, such as ϕ, can be elucidated analytically.

For completely hard (δ = 0) macromolecules, ϕ is trivially

$$\phi_0 = \frac{k}{n} \tag{4}$$

where the number of binding macromolecule is bounded above by $k = n$, as at this limit there are no available binding sites for a $k + 1$ incident macromolecule. For soft ($\delta > 0$) interactions, multiple macromolecules can occupy the same binding site and ϕ_0 is an upper bound to the actual volume fraction ϕ, i.e., $\phi \leq \phi_0$. Note that when $k > n$ the surface coverage concentration ϕ, which is the expectation value of ratio of occupied binding sites to total binding sites, cannot exceed unity. At the δ = 1 limit, the occupancy follows a binomial distribution

$$\begin{aligned}\phi &= 1 - \left(1 + \sum_{i=1}^{k} \binom{k}{i} \frac{(-\phi_0)^i}{k^i}\right) \\ &= 1 - \left(1 - \frac{\phi_0}{k}\right)^k\end{aligned} \tag{5}$$

which is bounded above by ϕ = 1. In the limit ($k \rightarrow \infty$, $n \rightarrow \infty$), eq 5 can be replaced with well-known Poisson distributed result,[63,64]

$$\phi = 1 - e^{-\phi_0} \tag{6}$$

which is the volume fraction occupied by macromolecules that overlap with no energy cost at the thermodynamic limit. Figure 1 shows selected configurations generated as macromolecules are sequentially added to binding sites with δ = 1. The softness of the macromolecules allows multiple occupancy of a binding site and causes a decrease in the occupied volume fraction with respect to ϕ_0.

At intermediate softness, $0 < \delta < 1$, the pairwise interactions generate complex behavior in ϕ. In the following two sections of this article, we will derive two expressions to predict the volume of a substrate occupied by an incident molecular species undergoing SSA.

3. EXACT OCCUPIED VOLUME FRACTION

Consider the sequential addition of k macromolecules added to a substrate with n binding sites. As the particles arrive at the substrate, the probability of selection for a specific site is $1/n$. In the nontrivial $\delta > 0$ regime, after the sequential addition of k macromolecules, the configurations of occupied sites that can be generated are given by the integer partitions $\{\nu_k\}$ of k. Kindt has developed theory to predict the equilibrium cluster size distribution of aggregating monomers using compositions of integers and separable partition functions,[5] and we modify his notation for our study. The partitions $\{\nu_k\}$ define a distinct set of occupied configurations (OC) that can be generated. For example, after the addition of 3 macromolecules the allowed OC are $\{\nu_3\}_1 = \{1, 1, 1\}$, $\{\nu_3\}_2 = \{2, 1\}$, and $\{\nu_3\}_3 = \{3\}$ (note that $\{2, 1\} = \{1, 2\}$). In general, the occupied binding sites take on configurations $\{\nu_k\}_i$ where $i \in \{1, 2, ..., p(k)\}$ and $p(k)$ is the number of partitions for the integer k. An estimation of $p(k)$,[65] for large k, is

$$p(k) \approx \frac{1}{4k\sqrt{3}} e^{\pi\sqrt{2k/3}} \tag{7}$$

Figure 2 shows the event graph $\mathcal{G}$, encompassing all possible OC that can be generated, for the sequential addition of k = 4 macromolecules. The first macromolecule k_0 added to the system must axiomatically bind to an unoccupied site and thus generate $\{\nu_1\}_1 = \{1\}$. This event is marked by letter "U" in

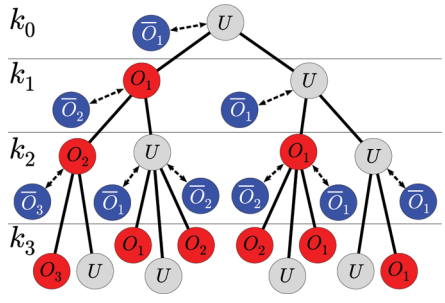

Figure 2. Avoidance-modified event graph $\mathcal{G}$ for the sequential addition $k_0 \rightarrow k_1 \rightarrow k_2 \rightarrow k_3$ of four macromolecules added to a solid substrate. The symbol O_i (red) represents that the macromolecule is accepted onto a binding site occupied by i macromolecules and $\bar{O}_i$ (blue) represents that the macromolecule is rejected from a site occupied by i macromolecules. In the event of rejection, a new site is selected, without memory, and the acceptance−avoidance site selection is repeated. Rejection events are shown as a directed dashed lines. An acceptance of the macromolecule by an unoccupied site is represented by U (gray).

dx.doi.org/10.1021/jp505207h | J. Phys. Chem. B 2014, 118, 14092−14102

Figure 2. The second macromolecule k_1 can bind to an unoccupied site (U) generating $\{\nu_2\}_1 = \{1, 1\}$, bind to the site occupied by the first macromolecule (event "O_1") generating $\{\nu_2\}_2 = \{2\}$, or be rejected by the site occupied by the first macromolecule (event "$\bar{O}_1$"). If macromolecule k_1 is rejected from the substrate, a new round of acceptance−rejection is begun; thus the only possible final states for k_1 are O_1 and U. Excluding the intermediate rejection outcomes, the third macromolecule k_2 has three possible final states. If the substrate is in configuration $\{\nu_2\}_1$, the macromolecule can bind to an unoccupied site (U) generating $\{\nu_3\}_1 = \{1, 1, 1\}$ or be accepted by either of the two occupied sites ("O_1") generating $\{\nu_3\}_2 = \{2, 1\}$. If the substrate is in configuration $\{\nu_2\}_2$, the macromolecule can bind to an unoccupied site (U) generating $\{\nu_3\}_2 = \{2, 1\}$ or be accepted by the site doubly occupied by the previously added macromolecules (O_2) generating $\{\nu_3\}_3 = \{3\}$. As illustrated in Figure 2, the fourth macromolecule k_3 has an increased complexity of available final states, which have a non-Markovian property, depending on all the previous states and on the possible intermediate rejection outcomes.

Let $\{\omega_k\}_i$ represent the occupancy vector of the partition $\{\nu_k\}_i$,

$$\{\omega_k\}_i = \{o_1, o_2, o_3, ..., o_k\} \tag{8}$$

where o_l is the number of sites with l bound macromolecules. For $k = 3$, the occupancy vectors are $\{\omega_3\}_1 = \{3, 0, 0\}$, $\{\omega_3\}_2 = \{1, 1, 0\}$, and $\{\omega_3\}_3 = \{0, 0, 1\}$. Coupled with the softness parameter δ, the occupancy vector defines a state polynomial,

$$S(\{\omega_k\}_i,\delta) = \sum_{l=1}^{k} o_l\delta^l \tag{9}$$

The normalized state polynomial

$$P_1(\mathrm{O}|\{\nu_k\}_i) = \frac{1}{n}S(\{\omega_k\}_i,\delta) \tag{10}$$

is the probability for the incident macromolecule to be accepted into any *occupied* state (event "O"), on the first round of acceptance−rejection, given that the OC of the substrate is $\{\nu_k\}_i$. Let $P_1(\bar{\mathrm{O}}\,|\,\{\nu_k\}_i)$ denote the conditional probability that the incident macromolecule is rejected by the substrate on the first round of acceptance−rejection, given that the OC of the substrate is $\{\nu_k\}_i$:

$$P_1(\bar{\mathrm{O}}|\{\nu_k\}_i) = \sum_{l=1}^{k} \frac{o_l}{n}(1 - \delta^l) \tag{11}$$

The probability of acceptance or rejection is the same for every round, but the probability to reach that round depends on the outcome of all previous rounds; e.g., the incident macromolecule can be accepted on the first round, rejected on the first round and accepted on the second, or rejected on the first and second and accepted on the third. This sequence continues *ad infinitum*, with each term in the sum representing a successive round of acceptance−rejection. The series is geometric, and thus the evaluated sum can be expressed as

$$P(\mathrm{O}|\{\nu_k\}_i) = P_1(\mathrm{O}|\{\nu_k\}_i)\frac{1}{1 - P_1(\bar{\mathrm{O}}|\{\nu_k\}_i)} \tag{12}$$

The conditional probability for an incident macromolecule to bind to any occupied site given that the substrate is in configuration $\{\nu_k\}_i$ can be expressed through the state polynomials (eqs 9 and 10),

$$P(\mathrm{O}|\{\nu_k\}_i) = \left(\frac{1}{n}\sum_{i=1}^{k} o_i\delta^i\right)\frac{1}{1 - \frac{1}{n}\sum_{i=1}^{k} o_i(1 - \delta^i)} = \frac{S(\{\omega_k\}_i,\delta)}{n - k + S(\{\omega_k\}_i,\delta)} \tag{13}$$

Accounting for all outcomes, the conditional probability to bind to an unoccupied site is

$$P(\mathrm{U}|\{\nu_k\}_i) = 1 - P(\mathrm{O}|\{\nu_k\}_i) \tag{14}$$

The probability given by eq 13 is a sum of the probabilities to bind to each occupied site j (event "O_j"),

$$P(\mathrm{O}|\{\nu_k\}_i) = \sum_{j=1}^{k} P(\mathrm{O}_j|\{\nu_k\}_i) \tag{15}$$

and thus the conditional probability for the $k + 1$ macromolecule to bind to a site occupied by j macromolecules is

$$P(\mathrm{O}_j|\{\nu_k\}_i) = \frac{o_j\delta^j}{n - k + S(\{\omega_k\}_i,\delta)} \tag{16}$$

The transition $\{\nu_k\}_i \rightarrow \mathrm{O}_j$ or $\{\nu_k\}_i \rightarrow \mathrm{U}$ generates a distinct partition $\{\nu_{k+1}\}_l$ of the $k + 1$ integer and thus the index l depends on j and must be included as an argument, $l = l(j)$. The index set $\{i, l\}$ defines a distinct node-to-node transition, and we arrive at the expression for the conditional probability that the $k + 1$ macromolecule added to the system generates the $\{\nu_{k+1}\}_{l(j)}$ partition, given that the previous k macromolecules are in the OC defined by $\{\nu_k\}_i$,

$$P_T(\{\nu_{k+1}\}_{l(j)}|\{\nu_k\}_i) = \frac{o_j\delta^j}{n - k + S(\{\omega_k\}_i,\delta)} \tag{17}$$

if the $k + 1$ macromolecule binds to an occupied site, or

$$P_T(\{\nu_{k+1}\}_{l(j)}|\{\nu_k\}_i) = 1 - \frac{S(\{\omega_k\}_i,\delta)}{n - k + S(\{\omega_k\}_i,\delta)} \tag{18}$$

if the $k + 1$ macromolecule binds to an unoccupied site.

Let $\mathcal{P}$ denote all the possible transition paths on the graph $\mathcal{G}$. A subset of $\mathcal{P}$ is $\mathcal{P}_i$ which is all the paths terminating at the configuration defined by the $\{\nu_k\}_i$th integer partition of k. The index set $\alpha = \{\alpha_1, \alpha_2, ..., \alpha_k\}$ is a subset of $\mathcal{P}_i$ and defines a specific path leading from the $\{\nu_1\}_1$ node to the $\{\nu_k\}_i$th node. The transition probability along a specific path α is the product of all the conditional node-to-node transition probabilities P_T on that path,

$$P_\alpha(\delta) = \prod_{j=1}^{k-1} P_T(\{\nu_{j+1}\}_{\alpha_{j+1}}\{\nu_j\}_{\alpha_j}) \tag{19}$$

The probability $P_\alpha(\delta)$ is a function of δ the softness parameter. A change in δ will alter the probability of a node-to-node transition in accordance with eq 13.

There are many such paths $\alpha \in \mathcal{P}_i$ and thus the probability to reach the $\{\nu_k\}_i$th state is the sum over all paths in $\mathcal{P}_i$,

$$P(\{\nu_k\}_i) = \sum_{\alpha\in\mathcal{P}_i}\prod_{j=1}^{k-1} P_T(\{\nu_{j+1}\}_{\alpha_{j+1}}|\{\nu_j\}_{\alpha_j}) \tag{20}$$

Equation 20 gives the probability to observe any configuration $\{\nu_k\}_i$.

dx.doi.org/10.1021/jp505207h | J. Phys. Chem. B 2014, 118, 14092−14102

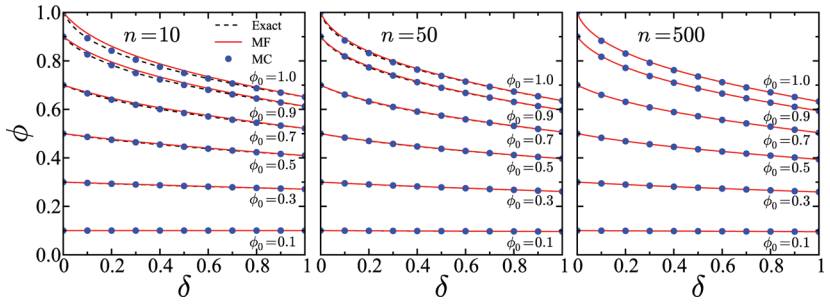

Figure 3. Fraction of occupied sites ϕ for different lattice sizes $n \in \{10, 50, 500\}$ from left to right, respectively, as a function of the softness parameter δ. The results for each lattice size are shown for various $\phi_0 = k/n$ values. Each circular marker (blue) is the result calculated from 10^6 Monte Carlo (MC) simulations. The exact solution given by eq 22, for each value of ϕ_0, is shown as a dashed curve (black). The results predicted by the continuum mean field (MF) approximation, given by eq 28 and presented in the next section, section 4, are shown as solid curves (red).

The fraction of substrate binding sites occupied by $\{\nu_k\}_i$ depends on its size. Let $\lambda(\{\nu_k\}_i)$ be a function that takes a partition as its argument and returns the size of that partition.

The occupied volume fraction of the ith partition is

$$\Phi(\{\nu_k\}_i) = \frac{\lambda(\{\nu_k\}_i)}{n} \tag{21}$$

which we enforce to be bounded from above at $\Phi = 1$. Combining eq 20 and eq 21 we obtain

$$\phi = \sum_{i=1}^{p(k)} \Phi(\{\nu_k\}_i) \left\{ \sum_{\alpha \in \mathcal{P}_i}^{\mathcal{P}_i \subseteq \mathcal{P}} \left(\prod_{j=1}^{k-1} P_T(\{\nu_{j+1}\}_{\alpha_{j+1}} | \{\nu_j\}_{\alpha_j}) \right) \right\} \tag{22}$$

which is the exact probability for a binding site to be occupied after the sequential addition of k macromolecules to n binding sites.

Shown in Figure 3 are the results for ϕ, given by eq 22, as a function of δ for various values of ϕ_0. For large ϕ_0 and small δ, ϕ is observed to rapidly decrease due to propensity for macromolecules to multiply occupy a site. The results from Monte Carlo (MC) simulations are shown as blue circular markers in Figure 3. The MC results for ϕ agree with those given by eq 22.

The site occupation distribution $P_X(x)$ can also be constructed from eq 20, where $x = 0$ corresponds to an unoccupied site, $x = 1$ is a site with one binding macromolecule, etc. For $x \geq 1$ this probability is

$$P_X(x) = \frac{1}{n} \sum_{i=1}^{p(k)} P(\{\nu_k\}_i) o_x \tag{23}$$

where o_x is the xth element of the occupancy vector for the partition $\{\nu_k\}_i$, defined by eq 8. The probability to observe an unoccupied site $(x = 0)$ is

$$\begin{aligned} P_X(0) &= 1 - \sum_{i=1}^{k} P_X(i) \\ &= 1 - \phi \end{aligned} \tag{24}$$

which is the remaining outcome after the probability for all occupied states has been counted.

Figure 4 shows the results for the distributions given by $P_X(x)$ as a function of ϕ_0 for various δ values. For $\delta = 0$ the system is completely hard and consists only of unoccupied and singly occupied sites. At $\delta = 0.025$ multiply occupied sites are allowed and the distribution is highly peaked as the system

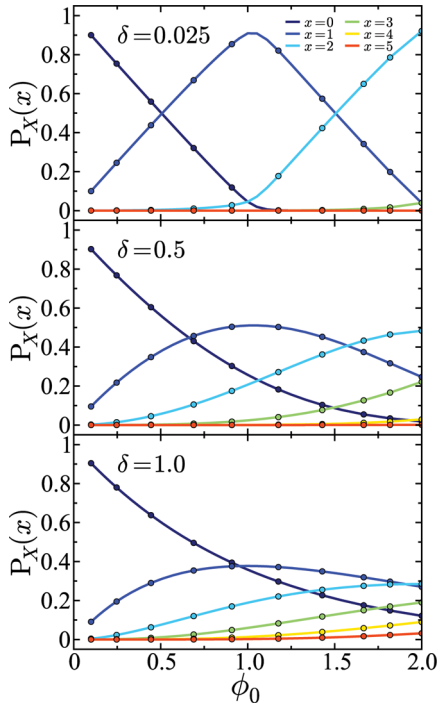

Figure 4. Distribution of site occupation $P_X(x)$ for $k = 20$ macromolecules as a function of ϕ_0. The exact results, given by eqs 23 and 24, for $\delta = 0.025$ (top), $\delta = 0.5$ (middle), and $\delta = 1$ (bottom) are shown as solid curves. Each circular markers is the result of 10^6 MC simulations.

enters clustering regimes at large ϕ_0. As δ is increased, sites that are multiply occupied become more probable and the distribution moves from a Poisson-like distribution at $\delta = 0.5$ to the exactly Poisson distribution at $\delta = 1$. Thus, the occupancy distributions can be separated into four regimes: the singly occupied HC limit at $\delta = 0$, the clustering regime at small δ, the Poisson-like regime at intermediate δ, and the exactly Poissonian limit at $\delta = 1$.

The scaling of $p(k)$ can be estimated by eq 7. As $(k \to \infty, n \to \infty)$ the exact expression for ϕ, given by eq 22, becomes intractable due to the large number of partitions that must accounted for in the calculation. Although, as shown in Figure 3, the values of ϕ at the thermodynamic limit are approached asymptotically, and the exact expression for ϕ gives a method to estimate ϕ for large k.

dx.doi.org/10.1021/jp505207h | J. Phys. Chem. B 2014, 118, 14092−14102

4. MEAN FIELD OCCUPANCY

In this section, we derive an expression built on MF arguments for the conditional probabilities to find multiply occupied sites. Herein, we refer to this approximation simply as the MF method. We have previously shown that expressions built on MF arguments can be used to accurately predict ϕ in off-lattice models where the dynamics are governed by stochastic bounded potentials. Full details of this derivation for a system of particles moving on a line can be found in ref 33, and for systems in higher dimensions in ref 34. We will generalize the MF expression for a system undergoing SSA as follows:

Let $Q^{(i)}$ denote the conditional probability that the ith macromolecule added to system, does not bind to a random site n_R given that $i - 1$ macromolecules have already been added. The occupied volume fraction after adding k macromolecules can be found as

$$\phi^{(k)} = 1 - \prod_{i=1}^{k} Q^{(i)} \tag{25}$$

The general probability of site n_R not being covered by the ith particle accounting for all possible configurations (single and multiple occupancy sites) of the previously added $i - 1$ macromolecules is

$$Q^{(i)} = \sum_{j=0}^{i-1} \binom{i-1}{j} \delta^{i-j-1}(1-\delta)^j q_j \tag{26}$$

The binomial coefficient $\binom{i-1}{j}$ counts the possible permutations of the jth configuration. The connection permutation probability q_j is the probability site n_R is not occupied by a newly added macromolecule given j macromolecules have already been placed in the system and that the newly added macromolecule interacts with the previously added macromolecules through the jth permutation of the interaction network. We find using MF arguments:[33]

$$q_j = \frac{q_0 - \phi^{(j)}}{1 - \phi^{(j)}} \tag{27}$$

with $q_0 = 1 - 1/n$. The conditional probability q_j accounts for each sequentially added macromolecule having a reduced number of binding sites available, with respect to those previously added. Only in the $\delta = 1$ limit is the available volume not reduced as every macromolecule is completely independent. Through eqs 26 and 27, ϕ can be expressed as

$$\phi^{\mathrm{MF}}(k,\delta) = 1 - \prod_{i=1}^{k}\left(\sum_{j=0}^{i-1} \binom{i-1}{j} \delta^{i-j-1}(1-\delta)^j q_j\right) \tag{28}$$

Equation 28 connects ϕ with the softness parameter δ. In the limiting values cases, $\delta = 0$ and $\delta = 1$, it leads to the exact results given by eqs 4 and 5, respectively.

The results of the MF approximation are shown in Figure 3. For small n, the MF method slightly overestimates ϕ. As the thermodynamic limit is approached ($k \to \infty$, $n \to \infty$) the MF method agrees with the exact result, given by eq 22, and with results obtained from MC simulations across all ranges of δ and ϕ_0.

5. RELAXED SURFACE COVERAGE (RSC) VS SSA

The creation−rejection−acceptance algorithm used to model sequential adsorption of macromolecules in the SSA procedure generates a distribution of energetic states, and hence spatial configurations, that are constrained to remain in place once trapped. This distribution will necessarily differ from the canonical Boltzmann distribution of states that results when the macromolecules are allowed to relax between sites after adsorption resulting in relaxed surface coverage. In this section, we will derive the equilibrium RSC distribution, use this distribution to calculate the equilibrium value of ϕ on a lattice, and compare this result with that generated from SSA. In a straightforward manner, we will first calculate the canonical partition function $Z(k,n,\beta)$ and use this to calculate the probability of observing a given state. The resulting equilibrium occupied volume fraction can be obtained through the assignment of the Boltzmann-weighted probability to the occupied volume fraction of each corresponding state.

We extend the notation of section 3 through the introduction of extended integer partitions, wherein the $\{\nu_k\}_i$th partition is appended with zeros such that the length of each extended partition $\{\mu_k\}_i$ is equal to n, i.e., $\lambda(\{\mu_k\}_i) = n$. For example, for $k = 3$ macromolecules binding to $n = 5$ sites, the allowed OC in the extended partition space are $\{\mu_3\}_1 = \{1, 1, 1, 0, 0\}$, $\{\mu_3\}_2 = \{2, 1, 0, 0, 0\}$, and $\{\mu_3\}_3 = \{3, 0, 0, 0, 0\}$ (cf. the OC described in section 3). We denote the jth element of the ith extended partition for the integer k as $\{\mu_k\}_i^j$.

The total number of overlapping contacts for each allowed OC, irrespective of the distribution (equilibrium or non-equilibrium), is given by

$$\mathcal{E}_i(\{\mu_k\}_i) = \frac{1}{2}\sum_{j=1}^{\lambda(\{\nu_k\}_i)} \{\mu_k\}_i^j(\{\mu_k\}_i^j - 1) \tag{29}$$

As the energy is pairwise additive, it is proportional to this quantity, i.e., E_i is given by $\epsilon\mathcal{E}_i(\{\mu_k\}_i)$ for the ith level. For $k \leq n$ the canonical partition function is

$$Z(k,n,\beta) = \sum_{i=1}^{p(k)} g_i(\{\mu_k\}_i)\mathrm{e}^{-\beta\epsilon\mathcal{E}_i(\{\mu_k\}_i)} \tag{30}$$

where g_i is the degeneracy of the ith extended partition. Note that the sum in eq 30 is over the integer partitions, not the energy levels themselves. In lattice-based systems, the calculation of the energy of each state is often trivial and consequently the determination of the degeneracy is often the principal hurdle in the evaluation of Z.[66,67] There is no contribution to the sum for $k > n$. This is a consequence of the fact there are no partitions of length greater than n because the length of such partitions would exceed the number of binding sites. Let $p(k,j)$ denote the number of integer partitions of k with exactly j parts. The sum of $p(k,j)$ over all $1 \leq j \leq k$ can then be denoted as $p(k)$, i.e.,

$$p(k) \equiv \sum_{j=1}^{k} p(k,j) \tag{31}$$

Let $\mathcal{K}$ denote the set of all integer partitions of k and $\mathcal{K}_j$ denote the set of integer partitions with exactly j parts: $\mathcal{K}_j \subseteq \mathcal{K}$. By restricting the sum in eq 30 over partitions with less than or equal to n parts, we arrive at the canonical partition function for all ϕ_0 values, including cases with $k > n$,

dx.doi.org/10.1021/jp505207h | J. Phys. Chem. B 2014, 118, 14092−14102

$$Z(k,n,\delta) = \sum_{j=1}^{n} \left(\sum_{\substack{i=1 \\ \{\nu_k\}_i \in \mathcal{K}_j}}^{p(k,j)} g_i(\{\mu_k\}_i) \delta^{\mathcal{E}_i(\{\mu_k\}_i)} \right) \tag{32}$$

We have substituted the exponential Boltzmann factors in eq 32 with the parameter δ, given by eq 2.

As noted previously, the total number of microstates for k distinguishable macromolecules binding to n distinguishable sites is n^k. For each set of partitions of length i, i.e., $\mathcal{K}_i$, we can thus sum over the size of each set through

$$n^k = \sum_{i=1}^{n} q^{\{p\}}(n,i)\, S_2(k,i) \tag{33}$$

where

$$q^{\{p\}}(n,i) = \frac{n!}{(n-i)!} \tag{34}$$

is a permutation operator and S_2 is a Stirling number of the second kind. In eq 33, each term in the sum is the number of microstates contributed to the total number of microstates by partitions of length i. We now need the number of permutations of each extended partition. Consider the number for ways of ordering k distinguishable macromolecules taken $\{\mu_k\}_i^1$, $\{\mu_k\}_i^2$, $\{\mu_k\}_i^3$, ..., $\{\mu_k\}_i^{\lambda(\{\nu_k\}_i)}$ at a time. The number of these permutations is given by

$$\begin{aligned} \mathcal{M}(\{\mu_k\}_i) &= \frac{k!}{\{\mu_k\}_i^1!\{\mu_k\}_i^2!\{\mu_k\}_i^3!\cdots\{\mu_k\}_i^k!} \\ &= k! \left(\prod_{j=1}^{\lambda(\{\nu_k\}_i)} \{\mu_k\}_i^j! \right)^{-1} \end{aligned} \tag{35}$$

The product in the denominator can be truncated at the index value $j = \lambda(\{\nu_k\}_i)$ as the remaining terms in the product are equal to unity. Let $\{\Omega_k\}_i$ represent the occupancy vector of the extended partition $\{\mu_k\}_i$,

$$\{\Omega_k\}_i = \{o_0, o_1, o_2, o_3, ..., o_k\} \tag{36}$$

where o_l is the number of sites with l bound macromolecules. Note that although the index of $\{\omega_k\}$ varies from 1 to k, the index of $\{\Omega_k\}$ varies from 0 to k. For $k = 3$ and $n = 5$, the occupancy vectors are $\{\Omega_3\}_1 = \{2, 3, 0, 0\}$, $\{\Omega_3\}_2 = \{3, 1, 1, 0\}$, and $\{\Omega_3\}_3 = \{4, 0, 0, 1\}$. We define a permutation operator

$$Q^{\{p\}}(\{\Omega_k\}_i) = \frac{n!}{o_0!o_1!o_3!\cdots o_k!} \tag{37}$$

that counts the permutations with repeated elements of $\{\Omega_k\}_i$. The degeneracy of the ith allowed partition belonging to $\mathcal{K}_j$ and its corresponding extended partition can therefore be expressed as

$$g_i(\{\mu_k\}_i) = \mathcal{M}(\{\mu_k\}_i)\, Q^{\{p\}}(\{\Omega_k\}_i) \tag{38}$$

For consistency, it can be verified that

$$\sum_{\substack{i=1 \\ \{\nu_k\}_i \in \mathcal{K}_j}}^{p(k,j)} g_i(\{\mu_k\}_i) = q^{\{p\}}(n,j)\, S_2(k,j) \tag{39}$$

and

$$\sum_{j=1}^{n} \left(\sum_{\substack{i=1 \\ \{\nu_k\}_i \in \mathcal{K}_j}}^{p(k,j)} g_i(\{\mu_k\}_i) \right) = n^k \tag{40}$$

Combining eqs 32 and 38, the equilibrium occupied volume fraction ϕ_E can be expressed as

$$\phi_E(k,n,\delta) = \sum_{j=1}^{j_{max}} \left(\sum_{\substack{i=1 \\ \{\nu_k\}_i \in \mathcal{K}_j}}^{p(k,j)} \Phi(\{\nu_k\}_i)\, g_i(\{\mu_k\}_i)\, \delta^{\mathcal{E}_i(\{\mu_k\}_i)} / Z(k,n,\delta) \right) \tag{41}$$

where $j_{max} = k$ if $k \leq n$ and $j_{max} = n$ otherwise. At the limiting values of δ, the well-known values for ϕ are recovered:

$$\lim_{\delta \to 0} \phi_E(k,n,\delta) = \begin{cases} \phi_0, & k \leq n \\ 1, & \text{otherwise} \end{cases} \quad \text{and}$$

$$\phi_E(k,n,1) = 1 - \left(1 - \frac{\phi_0}{k}\right)^k \tag{42}$$

To validate the analytical expression for ϕ_E, MC simulations were performed on systems with various values of δ, ϕ_0, and number of binding sites n. In these simulations, which were implemented using the Metropolis algorithm,[68,69] an initial random configuration was first relaxed to an equilibrium state by generating 10^6 configurations before a sampling phase was initiated. During the sampling phase, 10^6 configurations were generated. The ensemble average of these spatial states is the measured numerical result for ϕ_E. As shown in Figure 5, the results of these simulations are in excellent agreement with the result given by eq 41. For systems with $n = 2$ binding sites, the partition function is trivially solved and we employ this case to illustrate the variation of ϕ_E with n.

A comparison between the equilibrium results for ϕ_E, given by eq 41, and the nonequilibrium results for ϕ generated by the SSA procedure, and given by eq 22, are shown in Figure 5 for various system parameter values. At low densities ($\phi_0 \leq 0.5$) the equilibrium and SSA results are in close agreement but show increasing deviation as n is increased. In this density regime, a linear interpolation between ϕ values at the $\delta = 0$ and $\delta = 1$ limits was seen earlier to yield satisfactory results for systems governed by stochastic bounded potentials,[33] and this trend persists in the present lattice-based systems.

As the density of the system is increased, large deviations between the equilibrium and nonequilibrium SSA results are observed. At $\phi_0 = 1.0$, ϕ shows a convex functional shape because, for small values of δ, macromolecules are increasingly jammed into occupied sites. The result for the equilibrium RSC distribution is decreased with respect to the ϕ values generated by SSA. This decrease is caused by the propensity of macromolecules to move onto sites that are already occupied, increasing the number of multiple-occupation sites. In the SSA procedure this effect is absent as incident macromolecules bind irreversibly. For $\phi_0 = 1.5$, the system is overpacked as $k > n$. In this regime, macromolecules increasingly bind to already occupied sites, and ϕ shows a concave functional shape, differing sharply from cases with $\phi_0 \leq 1$. Interestingly, at large n, ϕ_E is an approximately linear function of δ and ϕ values generated by SSA continue to show strong nonlinear behavior.

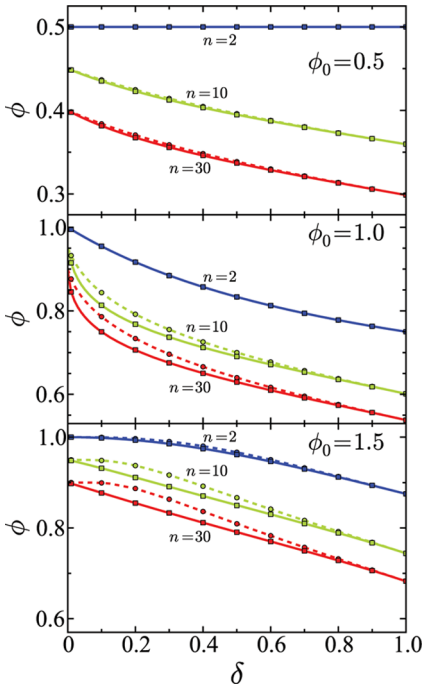

Figure 5. Fraction of occupied sites ϕ for ϕ_0 = 0.5 (top), ϕ_0 =1.0 (middle), and ϕ_0 = 1.5 (bottom) as a function of δ. For each value of ϕ_0, results are shown for n = 2 (blue), n = 10 (green), and n = 30 (red) binding sites. All results are shifted vertically by $\Delta\phi \in \{-0.05, -0.1\}$, when $n \in \{10, 30\}$, respectivelty, for visual clarity. The dashed curves are the analytical results, given by eq 22, for a system undergoing SSA. Each circular marker is the result of 10^6 MC simulations for a system undergoing SSA. The analytical RSC distribution, given by eq 41, is shown as a solid curve. Each square marker is the result measured from 10^6 configurations generated using the Metropolis MC algorithm for the RSC distribution.

6. OFF-LATTICE INTERACTIONS

On continuum state spaces, systems whose dynamics are governed by deterministic bounded potentials form metastable crystalline phases at high densities (large ϕ_0).[32,40,52,59] Bounded potentials have also been realized stochastically,[33] where the pairwise interaction between a set of particles i and j is described by the following equation:

$$V_{ij}^{S}(r) = \begin{cases} 0, & r > \sigma \\ 0, & r \le \sigma \text{ and } a_{ij}(t_{\text{col}}) < \delta \\ \infty, & r \le \sigma \text{ and } a_{ij}(t_{\text{col}}) > \delta \end{cases} \tag{43}$$

In dynamical simulations, eq 43 is implemented by generating a random number $a_{ij} \in [0, 1]$ at the time of collision t_{col} between particles i and j. If $a_{ij}(t_{\text{col}}) > \delta$, the particles interact via a hard (HC) potential and collide elastically; otherwise, the particles interpenetrate without interacting. As a_{ij} is generated each time the particles collide, the interaction (hard or ideal) between a set of particles can change many times throughout the simulation. In the potential given by eq 43, as in the SSA algorithm, δ is a softness parameter, bridging completely hard (δ = 0) and completely soft (δ = 1) behavior. At intermediate values ($0 < \delta < 1$), the mixing of hard collisions and soft ideal interactions generates complex spatial arrangements, including clustering regimes at large densities.[34]

To study the applicability of eq 22 to systems that include off-lattice interactions, molecular dynamics (MD) simulations[70] were performed on a system of k = 20 particles (disks) constrained to move on a periodic surface of area $\mathcal{A}$, with each particle having a diameter σ and mass m. The potential between each pair of particles in these simulations is given by eq 43. To assign the initial position of each particle, a uniform lattice was constructed in $\mathcal{A}$ and the center of each particle was placed on a distinct lattice site. The initial velocities were sampled from a Boltzmann distribution, and the system was then evolved through a time-driven hard-sphere algorithm[71] wherein the particles are treated as semihard disks moving on a two-dimensional surface. The underlying softness of the particle–particle interactions is adjusted through the parameter δ.

The MD simulations were performed in two phases. First, the system was spatially relaxed for 10^4 collisions. The relaxation phase was implemented to achieve an equilibrium structure. In the second phase, ϕ is measured using MC integration.[29,31,33,34] The MC integration approach involves generating a large number of random coordinates in $\mathcal{A}$ and checking if those coordinates are overlapped by any particle from the system. The ratio of sampling points that are overlapped to the total number of points generated is ϕ. For each parameter set $\{\delta,\phi_0\}$, 10^4 frames were integrated by generating 10^6 sampling points per frame. To confirm that the system is in an equilibrium state during this sampling phase, simulations were also performed with the initial positions of the particles chosen randomly. The results measured using random initial positions were in agreement with those measured using a uniform lattice as the initial configuration. The volume fraction ϕ_0 is the occupied volume fraction of the system when no particles overlap. On a continuum state space this volume fraction is $\phi_0 = kv/\mathcal{A}$ where $v = \pi\sigma^2/4$ is the area of a single disk. When the particles are allowed to overlap ($\delta > 0$), the observed volume fraction ϕ is less than ϕ_0.

The inclusion of off-lattice interactions generates a different distribution of states than those derived in eqs 22 and 28 due to the propensity for particles to be pushed into overlapping configurations by neighboring particles. To account for multibody effects in the distribution of spatial configurations, the pairwise softness parameter δ must be replaced with a multibody induced softness parameter ζ, which can be derived from the effective pairwise potential between two particles. We have previously shown that in these systems the softness parameter δ has a significant influence on the form of the radial distribution function $g(r)$[33,34] and therefore this distribution is parametrized by δ: $g(r) = g(r;\delta)$. The potential of mean force (PMF), denoted as $w(r;\delta)$, between a pair of particles acts along the line connecting their centers and can expressed through $g(r;\delta)$ from the relationship

$$g(r;\delta) = \mathrm{e}^{-\beta w(r;\delta)} \tag{44}$$

where $\beta = 1/k_{\text{B}}T$. An integral of $\mathrm{e}^{-\beta w(r;\delta)}$ over the diameter of a single particle (the region where overlaps occur) is a sum of Boltzmann-weighted pairwise configurations, induced by interactions with all other particles in the system. The ratio of this multibody induced distribution to the ideal (δ = 1) distribution

$$\zeta(\delta) = \frac{\int_0^\sigma \mathrm{e}^{-\beta w(r;\delta)}\,\mathrm{d}r}{\int_0^\sigma \mathrm{e}^{-\beta w(r;1)}\,\mathrm{d}r} \tag{45}$$

defines ζ. The mapping $\delta \to \xi$ must be used in eqs 22 and 28 to account for off-lattice interactions.

dx.doi.org/10.1021/jp505207h | J. Phys. Chem. B 2014, 118, 14092–14102

Figure 6 shows the results for ϕ given by the lattice model and the MF model, both with ζ mapping, and the results

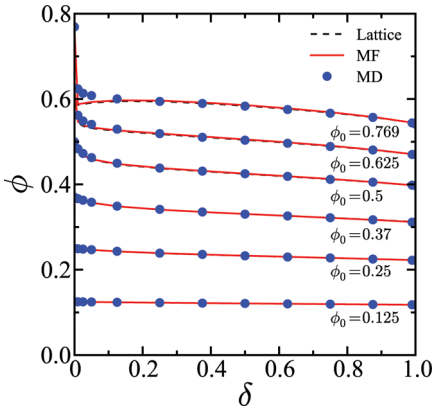

Figure 6. Occupied volume fraction ϕ as a function of the softness parameter δ for a system with included off-lattice interactions. The filled circles (blue) are the results measured from MD simulations. The dashed curves (black) are the results of the lattice model, obtained by combining eqs 22 and 45, The solid curves (red) are the results from the continuum MF method given by eqs 28 and 45.

measured from MD simulations. The results are in excellent agreement apart from the small-δ (<0.05), large-ϕ_0 (=0.769) regime. The compared theoretical expressions account only for acceptance and rejection outcomes, and in this regime the PMF has attractive sections and forms metastable wells in the overlapping region ($0 \leq r < \sigma$), causing deviation. The well depth of the PMF in the overlapping region, $\Delta V = w(\sigma^-;\delta) - w(0;\delta)$, increases at higher densities and lower δ values. For $\phi_0 = 0.25$ and $\delta = 0.75$, $\Delta V \approx 0.03\ k_BT$, whereas for $\delta = 0.01$, $\Delta V \approx 0.9\ k_BT$. At the highest density studied, $\phi_0 = 0.769$, for $\delta = 0.75$, $\Delta V \approx 0.1\ k_BT$ and for $\delta = 0.01$, $\Delta V \approx 5\ k_BT$. Thus, at large densities and small interparticle softness, a distinct transition to a cluster-forming regime is observed. The deviations between the MF results and the results measured from MD simulations, as shown in Figure 6, are caused by this phase transition which is not included in the derivation of eq 28. This clustering phenomenon is in agreement with that previously observed in systems governed by deterministic[38] and stochastic[34] bounded potentials. As δ is moved slightly from the $\delta = 0$ limit, ϕ decreases drastically due to pressure pushing the particles into overlapped states. As higher densities are approached, the lattice model gives a slightly better prediction of ϕ with respect to the MF model. This is expected, as configurations on the continuum become more lattice-like when the available free volume for each particle decreases.

7. CONCLUSIONS

Motivated by the design of mesoscale devices with unique functionalities, we have obtained analytic and numerical relationships for the characteristic surface coverage in the sequential adsorption of soft macromolecules to a solid substrate with discrete binding sites. The exact fraction of occupied binding sites ϕ and the site occupancy distributions have been solved exactly for a developed avoidance-modified multiple occupancy model. The results of this derivation have been confirmed by comparison with Monte Carlo (MC) simulations. Due to the complexity of the exact expression at the thermodynamic limit, a mean field (MF) derivation for ϕ was presented and compared with the exact result and results measured from MC simulations. We have found that as the thermodynamic limit is approached, the MF expression converges to the exact result. Moreover, we conjecture that the MF expression is exact at the thermodynamic limit for a system consisting of discrete binding sites.

The inclusion of off-lattice interactions was realized using a stochastic bounded potential which allows multiple macromolecules to occupy the same volume in a continuum configuration space. Molecular dynamics (MD) simulations were performed on a system of macromolecules confined to move on a surface under the influence of a stochastic bounded potential. The fraction of configuration space occupied by the particle phase of the system was measured and compared with the results given the exact and MF expressions derived for the on-lattice sequential adsorption procedure. We find excellent agreement between these results, which provides evidence that, at the mesoscale, spatial configurations generated through avoidance-modified sequential addition processes can be smoothly mapped to the spatial configurations of a system in thermodynamic equilibrium. The relaxed surface coverage mechanism following the SSA has also been obtained directly from theory, confirmed by simulation, and seen to lead to reduced occupied volume fractions.

The results presented in this article elucidate the range of clustering behavior and accessible structural configurations due to the soft and complex fluid interactions. Such interactions can arise at the mesoscopic length scales of computational models when the forces acting on atomistic degrees of freedom are coarse-grained. Fabrication processes involving the adsorption of particles on a surface can generally be modeled through the stacking of nonoverlapping building blocks. The present work includes the possibility that the interparticle interactions are soft enough to allow overlaps. Fabrication utilizing such particles could thus lead to very different kinds of assemblies (with larger effective densities) and may be useful in creating new devices.

AUTHOR INFORMATION

Corresponding Author

*R. Hernandez. E-mail: hernandez@gatech.edu.

Notes

The authors declare no competing financial interest.

ACKNOWLEDGMENTS

This work has been partially supported by the National Science Foundation (NSF) through Grant No. NSF-CHE-1112067. We also thank Prof. Mostafa El-Sayed for his insight and support of our work.

REFERENCES

(1) Stubbs, J. M.; Siepmann, J. I. Aggregation in Dilute Solutions of 1-Hexanol in *n*-Hexane: A Monte Carlo Simulation Study. *J. Phys. Chem. B* **2002**, *106*, 3968−3978.

(2) Duff, N.; Peters, B. Nucleation in a Potts Lattice Gas Model of Crystallization from Solution. *J. Chem. Phys.* **2009**, *131*, 184101.

(3) Sanders, S. A.; Panagiotopoulos, A. Z. Micellization Behavior of Coarse Grained Surfactant Models. *J. Chem. Phys.* **2010**, *132*, 114902.

(4) Georgiadis, C.; Moultos, O.; Gergidis, L. N.; Vlahos, C. Brownian Dynamics Simulations on the Self-Assembly Behavior of AB Hybrid Dendritic-Star Copolymers. *Langmuir* **2011**, *27*, 835−842.

(5) Kindt, J. T. Accounting for Finite-Number Effects on Cluster Size Distributions in Simulations of Equilibrium Aggregation. *J. Chem. Theory Comput.* **2013**, *9*, 147−152.

(6) Poon, G. G.; Peters, B. A Stochastic Model for Nucleation in the Boundary Layer during Solvent Freeze-Concentration. *Cryst. Growth Des.* **2013**, *13*, 4642−4647.
(7) Agarwal, V.; Peters, B. Nucleation Near the Eutectic Point in a Potts-Lattice Gas Model. *J. Chem. Phys.* **2014**, *140*, 084111.
(8) Glotzer, S. C. Some Assembly Required. *Science* **2004**, *306*, 419.
(9) Glotzer, S. C.; Solomon, M. J. Anisotropy of Building Blocks and Their Assembly into Complex Structures. *Nat. Mater.* **2007**, *6*, 557−562.
(10) Hagy, M. C.; Hernandez, R. Dynamical Simulation of Dipolar Janus Colloids: Equilibrium Structure and Thermodynamics. *J. Chem. Phys.* **2012**, *137*, 044505.
(11) Hagy, M. C.; Hernandez, R. Dynamical Simulation of Electrostatic Striped Colloidal Particles. *J. Chem. Phys.* **2014**, *140*, 034701.
(12) Marrink, S. J.; Risselada, H. J.; Yefimov, S.; Tieleman, D. P.; de Vries, A. H. The MARTINI Force Field: Coarse Grained Model for Biomolecular Simulations. *J. Phys. Chem. B* **2007**, *111*, 7812−7824.
(13) Lyubimov, I.; Guenza, M. G. First-Principle Approach to Rescale the Dynamics of Simulated Coarse-Grained Macromolecular Liquids. *Phys. Rev. E* **2011**, *84*, 031801.
(14) Dama, J. F.; Sinitskiy, A. V.; McCullagh, M.; Weare, J.; Roux, B.; Dinner, A. R.; Voth, G. A. The Theory of Ultra-Coarse-Graining. 1. General Principles. *J. Chem. Theory Comput.* **2013**, *9*, 2466−2480.
(15) Saunders, M. G.; Voth, G. A. Coarse-Graining Methods for Computational Biology. *Annu. Rev. Biophys.* **2013**, *42*, 73−93.
(16) Noid, W. G. Perspective: Coarse-Grained Models for Biomolecular Systems. *J. Chem. Phys.* **2013**, *139*, 090901.
(17) Likos, C. N. Effective Interactions in Soft Condensed Matter Physics. *Phys. Rep.* **2001**, *348*, 267−439.
(18) Mladek, B. M.; Kahl, G.; Neumann, M. Thermodynamically Self-Consistent Liquid State Theories for Systems With Bounded Potentials. *J. Chem. Phys.* **2006**, *124*, 064503.
(19) Stillinger, F. Phase Transitions in the Gaussian Core System. *J. Chem. Phys.* **1976**, *65*, 3968−3974.
(20) Likos, C. N.; Rosenfeldt, S.; Dingenouts, N.; Ballauff, M.; Lindner, P.; Werner, N.; Vogtle, F. Gaussian Effective Interaction Between Flexible Dendrimers of Fourth Generation: A Theoretical and Experimental Study. *J. Chem. Phys.* **2002**, *117*, 1869−1877.
(21) Graf, H.; Löwen, H. Density Jumps Across Phase Transitions in Soft-Matter Systems. *Phys. Rev. E* **1998**, *57*, 5744−5753.
(22) Schmidt, M.; Fuchs, M. Penetrability in Model Colloid−Polymer Mixtures. *J. Chem. Phys.* **2002**, *117*, 6308−6312.
(23) Pamies, J. C.; Cacciuto, A.; Frenkel, D. Phase Diagram of Hertzian Spheres. *J. Chem. Phys.* **2009**, *131*, 044514.
(24) Wang, Q. Studying Soft Matter with "Soft" Potentials: Fast Lattice Monte Carlo Simulations and Corresponding Lattice Self-consistent Field Calculations. *Soft Matter* **2009**, *5*, 4564−4567.
(25) Wang, Q. Theory and Simulation of the Self-Assembly of Rod-Coil Block Copolymer Melts: Recent Progress. *Soft Matter* **2011**, *7*, 3711−3716.
(26) Pötschke, D.; Ballauff, M.; Lindner, P.; Fischer, M.; Vögtle, F. The Structure of Sendritic Molecules in Solution as Investigated by Small-Angle Neutron Scattering. *Macromol. Chem. Phys.* **2000**, *201*, 330−339.
(27) Ballauff, M.; Likos, C. N. Dendrimers in Solution: Insight from Theory and Simulation. *Angew. Chem., Ind. Ed.* **2004**, *43*, 2998−3020.
(28) Torquato, S.; Stell, G. Microstructure of Two-Phase Random Media. IV. Expected Surface Area of a Dispersion of Penetrable Spheres and Its Characteristic Function. *J. Chem. Phys.* **1984**, *80*, 878−880.
(29) Lee, S.; Torquato, S. Porosity for the Penetrable-Concentric-Shell Model of Two-phase Disordered Media: Computer Simulation Results. *J. Chem. Phys.* **1988**, *89*, 3258−3263.
(30) Suh, S.; Min, W.; MacElroy, J. Simulation Studies for Porosity and Specific Surface Area in the Penetrable-Concentric-Shell Model Pore. *Bull. Korean Chem. Soc.* **1999**, *20*, 1521−1523.
(31) Elsner, A.; Wagner, A.; Aste, T.; Hermann, H.; Stoyan, D. Specific Surface Area and Volume Fraction of the Cherry-Pit Model with Packed Pits. *J. Phys. Chem. B* **2009**, *113*, 7780−7784.
(32) Suh, S.; Kim, C.; Kim, S.; Santos, A. Molecular Dynamics Simulation Study of Self-Diffusion for Penetrable-Sphere Model Fluids. *Phys. Rev. E* **2010**, *82*, 051202.
(33) Craven, G. T.; Popov, A. V.; Hernandez, R. Stochastic Dynamics of Penetrable Rods in One Dimension: Occupied Volume and Spatial Order. *J. Chem. Phys.* **2013**, *138*, 244901.
(34) Craven, G. T.; Popov, A. V.; Hernandez, R. Structure of a Tractable Stochastic Mimic of Soft Particles. *Soft Matter* **2014**, *10*, 5350−5361.
(35) Mattsson, J.; Wyss, H. M.; Fernandez-Nieves, A.; Miyazaki, K.; Hu, Z.; Reichman, D. R.; Weitz, D. A. Soft Colloids Make Strong Glasses. *Nature* **2009**, *462*, 83−86.
(36) Tonks, L. The Complete Equation of State of One, Two and Three-Dimensional Gases of Hard Elastic Spheres. *Phys. Rev.* **1936**, *50*, 955−963.
(37) Mladek, B. M.; Gottwald, D.; Kahl, G.; Neumann, M.; Likos, C. N. Formation of Polymorphic Cluster Phases for a Class of Models of Purely Repulsive Soft Spheres. *Phys. Rev. Lett.* **2006**, *96*, 045701.
(38) Mladek, B. M.; Charbonneau, P.; Likos, C. N.; Frenkel, D.; Kahl, G. Multiple Occupancy Crystals Formed by Purely Repulsive Soft Particles. *J. Phys.: Condens. Matter* **2008**, *20*, 494245.
(39) Zhang, K.; Charbonneau, P. [N]pT Monte Carlo Simulations of the Cluster-Crystal-Forming Penetrable Sphere Model. *J. Chem. Phys.* **2012**, *136*, 214106.
(40) Coslovich, D.; Ikeda, A. Cluster and Reentrant Anomalies of Nearly Gaussian Core Particles. *Soft Matter* **2013**, *9*, 6786−6795.
(41) Feder, J. Random Sequential Adsorption. *J. Theor. Biol.* **1980**, *87*, 237−254.
(42) Widom, B. Random Sequential Addition of Hard Spheres to a Volume. *J. Chem. Phys.* **1966**, *44*, 3888−3894.
(43) Torquato, S.; Uche, O. U.; Stillinger, F. H. Random Sequential Addition of Hard Spheres in High Euclidean Dimensions. *Phys. Rev. E* **2006**, *74*, 061308.
(44) Cieśla, M. Continuum Random Sequential Adsorption of Polymer on a Flat and Homogeneous Surface. *Phys. Rev. E* **2013**, *87*, 052401.
(45) Cieśla, M. Random Sequential Adsorption of Tetramers. *J. Stat. Mech.* **2013**, *2013*, P07011.
(46) Jin, X.; Wang, N. H. L.; Tarjus, G.; Talbot, J. Irreversible Adsorption on Nonuniform Surfaces: The Random Site Model. *J. Phys. Chem.* **1993**, *97*, 4256−4258.
(47) Talbot, J.; Tarjus, G.; Viot, P. Equilibrium Adsorption on a Random Site Surface. *J. Phys. Chem. B* **2008**, *112*, 13051−13058.
(48) Langmuir, I. The Constitution and Fundamental Properties of Solids and Liquids. Part I. Solids. *J. Am. Chem. Soc.* **1916**, *38*, 2221−2295.
(49) Brunauer, S.; Emmett, P. H.; Teller, E. Adsorption of Gases in Multimolecular Layers. *J. Am. Chem. Soc.* **1938**, *60*, 309−319.
(50) Masel, R. I. *Principles of Adsorption and Reaction on Solid Surfaces*; John Wiley & Sons: New York, 1996.
(51) Finken, R.; Hansen, J.-P.; Louis, A. A. Phase Separation of a Multiple Occupancy Lattice Gas. *J. Phys. A* **2004**, *37*, 577.
(52) Likos, C.; Watzlawek, M.; Löwen, H. Freezing and Clustering Transitions for Penetrable Spheres. *Phys. Rev. E* **1998**, *58*, 3135−3144.
(53) Rottgermann, P. J. F.; Alberola, A. P.; Radler, J. O. Cellular Self-Organization on Micro-Structured Surfaces. *Soft Matter* **2014**, *10*, 2397−2404.
(54) Lin, C.-C.; Anseth, K. S. Cell-Cell Communication Mimicry with Poly(Ethylene Glycol) Hydrogels for Enhancing β-Cell Function. *Proc. Natl. Acad. Sci. U. S. A.* **2011**, *108*, 6380−6385.
(55) Santos, A.; Malijevskỳ, A. Radial Distribution Function of Penetrable Sphere Fluids to the Second Order in Density. *Phys. Rev. E* **2007**, *75*, 021201.
(56) Malijevskỳ, A.; Yuste, S.; Santos, A. Low-temperature and High-temperature Approximations for Penetrable-sphere Fluids: Compar-

ison with Monte Carlo Simulations and Integral Equation Theories. *Phys. Rev. E* **2007**, *76*, 021504.
(57) Malijevsky, A.; Santos, A. Structure of Penetrable-Rod Fluids: Exact Properties and Comparison Between Monte Carlo Simulations and Two Analytic Theories. *J. Chem. Phys.* **2006**, *124*, 074508.
(58) Choudhury, N.; Ghosh, S. Integral Equation Theory of Penetrable Sphere Fluids: A Modified Verlet Bridge Function Approach. *J. Chem. Phys.* **2003**, *119*, 4827−4832.
(59) Viererblová, L.; Kolafa, J.; Labk, S.; Malijevskỳ, A. Virial Coefficients and Equation of state of the Penetrable Sphere Model. *Phys. Chem. Chem. Phys.* **2010**, *12*, 254−262.
(60) Marquest, C.; Whitten, T. Simple Cubic Structure in Copolymer Mesophases. *J. Phys. (Paris)* **1989**, *50*, 1267−1277.
(61) Li, H.; Qian, C.-J.; Wang, C.; Luo, M.-B. Critical Adsorption of a Flexible Polymer Confined Between Two Parallel Interacting Surfaces. *Phys. Rev. E* **2013**, *87*, 012602.
(62) Milchev, A.; Egorov, S. A.; Binder, K. Critical Adsorption of a Single Macromolecule in Polymer Brushes. *Soft Matter* **2014**, 5974−−5990.
(63) Quintanilla, J.; Torquato, S. Clustering Properties of *d*-Dimensional Overlapping Spheres. *Phys. Rev. E* **1996**, *54*, 5331−5339.
(64) Torquato, S.; Lu, B.; Rubinstein, J. Nearest-Neighbor Distribution Functions in Many-Body Systems. *Phys. Rev. A* **1990**, *41*, 2059−2075.
(65) Hardy, G. H.; Ramanujan, S. Asymptotic Formulae in Combinatory Analysis. *Proc. London Math. Soc.* **1918**, *2*, 75−115.
(66) Vavro, J. Exact Solution for the Lattice Gas Model in One Dimension. *Phys. Rev. E* **2001**, *63*, 057104.
(67) Yilmaz, M. B.; Zimmermann, F. M. Exact Cluster Size Distribution in the One-Dimensional Ising Model. *Phys. Rev. E* **2005**, *71*, 026127.
(68) Metropolis, N.; Rosenbluth, A. W.; Rosenbluth, M. N.; Teller, A. H.; Teller, E. Equation of State Calculations by Fast Computing Machines. *J. Chem. Phys.* **1953**, *21*, 1087−1092.
(69) Frenkel, D.; Smit, B. *Understanding Molecular Simulation: From Algorithms to Application*; Academic Press: New York, 1996.
(70) Hernandez, R.; Popov, A. Molecular Dynamics Out of Equilibrium: Mechanics and Measurables. *Wiley Interdiscip. Rev.: Comput. Mol. Sci.* **2014**, DOI: 10.1002/wcms.1190.
(71) Allen, M. P.; Tildesley, D. J. *Computer Simulations of Liquids*; Oxford: New York, 1987.